

Electronically Steerable Parasitic Array Radiator Flush-Mounted for Automotive LTE

Gerald Artner¹, Jerzy Kowalewski², Jude Atuegwu², Christoph F. Mecklenbräuer¹, Thomas Zwick²

¹Institute of Telecommunications, Technische Universität Wien, Vienna, Austria, gerald.artner@nt.tuwien.ac.at

²Institute of Radio Frequency Engineering and Electronics, Karlsruhe Institute of Technology, Karlsruhe, Germany.

Abstract—A pattern reconfigurable antenna for 2.6 GHz LTE is flush-mounted in a chassis antenna cavity. The driven element is a top-loaded monopole, that is steered based on the electronically steerable parasitic array radiator (ESPAR) principle. The radiation pattern can be configured in 45 degree steps, e.g. front, diagonal front-right, right, etc. The cavity prototype is made from carbon fiber reinforced polymer and includes a chassis mockup. Antenna performance is evaluated based on measured gain patterns, which show that the antenna retains its reconfiguration capabilities when it is flush-mounted. Further, a parametric measurement study with regards to antenna height inside the cavity is performed to investigate the option of mounting an electronics module underneath the antenna.

Index Terms—antenna, automotive, cavity, ESPAR, flush-mounted, measurement, reconfigurable, vehicular.

I. INTRODUCTION

The orientation of vehicles towards base stations is initially considered to be unknown. For the past decades the goal of automotive antenna design was therefore to achieve omnidirectional radiation patterns [1]. However, once the vehicle is connected to a specific base station it is desirable to steer a beam in the direction of the base station or a strong multipath component. In automotive applications, the beam steering is done with pattern reconfigurable antennas that use pin-diodes or micro-electromechanical systems (MEMS), as they meet the requirements for fast switching and temperature stability. Pattern reconfigurable antennas for the automotive environment are presented in [2], [3].

Vehicular antennas are increasingly moved away from protruding modules when the aesthetic appearance is important, and to reduce the drag coefficient – and therefore fuel consumption. Transparent antennas can be applied to vehicle windows, which is already state of the art for radio antennas on the rear windows [4], [5]. Finer metal meshes allow more complex geometries [6]. A promising paradigm is to build flush-mounted antennas inside cavities in the chassis [7], [8], [9], [10]. Such cavities can be manufactured as part of the car roof [11], [12], [13]. Smaller cavities have been proposed for flush-mounted antennas in the monocoque of racing cars [14].

Few antennas have been proposed that are suited for automotive applications, hidden and pattern reconfigurable. [15], [16] investigate such antennas based on phased driven elements inside chassis cavities. A pattern reconfigurable antenna integrated in the rear view mirror is demonstrated in [17]. The antenna is based on the theory of characteristic modes.

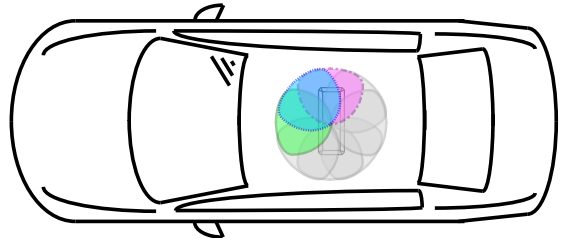


Fig. 1: Exemplary location of an ESPAR flush-mounted in a chassis antenna cavity. The beam can be reconfigured in steps of 45°.

Contribution — A pattern reconfigurable antenna for 2.6 GHz LTE is flush-mounted in a chassis antenna cavity. It is designed as ESPAR that allows beam steering in 45° steps. Fig. 1 shows a possible position of the antenna in the center of a car roof. The cavity prototype is built with a chassis-mockup as carbon fiber reinforced polymer (CFRP) laminate. Calibrated gain patterns are measured in an anechoic chamber. Additionally, a parametric measurement study is performed to quantify the influence of mounting height inside the cavity, e.g. to place electronics modules underneath the antenna.

II. ANTENNA DESIGN

The pattern reconfigurable antenna was first described in [18]. The antenna is a three-dimensional structure that is erected from a ground plane manufactured in printed circuit board (PCB) technology. The ground plane is a 500 mm × 500 mm FR-4 substrate with thickness 1.6 mm and permittivity $\epsilon_r = 4.3$. The driven element of the antenna is a vertical post in its center. To reduce the height of the antenna, the quarter-wavelength long post is top-loaded capacitively with a perpendicular metal square with a side length of 13 mm. This reduces the post height from $\lambda/4$ to $\lambda/10$. Switchable parasitic elements are then added to design an electronically steerable parasitic array radiator (ESPAR). Four top-loaded parasitic posts are added around the driven post. Two wires are used to short each parasitic element to the ground in order to improve the antenna matching and the gain. The shorting wires are moved to the edge of the parasitic element to reduce the coupling between the driven and parasitic element and further improve the gain. To increase the mechanical stability of the antenna, all top-loading elements are combined on a second PCB. Therefore, the height of the parasitic

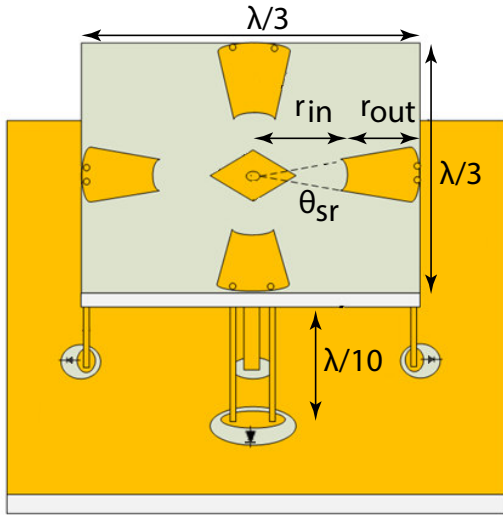


Fig. 2: Geometry of the ESPAR antenna. Image reused from [18].

elements is fixed to the height of the driven element. To reduce losses, the PCB for the top-loading elements is built from a Rogers RT5880 substrate with a thickness of 0.508 mm and permittivity $\epsilon_r = 2.2$. Sector-ring geometries are chosen for the top-loading of the parasitic elements, because their alignment around the driven element is circularly symmetric. The resonance frequency of the parasitic elements is designed to be slightly lower than that of the driven element, such that they can act as resonant reflectors. The opening angle of the ring sectors $\theta_{sr} = 17^\circ$, their inner radii $r_{in} = 12$ mm and their outer radii $r_{out} = 10$ mm are found numerically by simulation. Reducing r_{in} increases the resonance frequency and the bandwidth, it improves impedance matching as well (up to some point). The antenna geometry is shown in Fig. 2.

The parasitic elements can be configured as either reflector or director, by connecting their electric potential to ground or letting it float. This is done with pin-diodes connected to the ground plane on the bottom PCB. A parasitic element is configured as reflector when its electric potential is connected to ground, which is done by activating its diode on the bottom PCB. When the diode is switched on, the current on the parasitic element post is approximately -80° out of phase with the current on the driven post. With a distance of 0.14λ between driven and parasitic element, this results in destructive interference towards the parasitic element and constructive interference towards the driven element, i.e. the parasitic element acts as a reflector. A parasitic element is configured as a director when its electric potential floats (i.e. it is not connected to ground), which is done by deactivating the diode on the bottom PCB. The current on the parasitic element post is then approximately 140° out of phase with the driven post. The DC biasing for the pin-diodes is done via a resistor in order to block the RF signal from the DC supply. A choice of $5\text{ k}\Omega$ for the resistor allows to switch the diodes on and off with 5 V and 0 V, respectively. Which means that

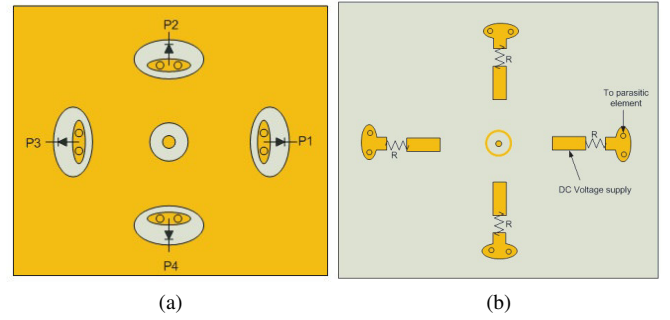


Fig. 3: PCB layout on the ground plane with pin-diodes and biasing circuit for switching the parasitic elements: a) top view and b) bottom view. Images reused from [18].

the switching can be done with 5 V logic voltage levels, e.g. transistor-transistor logic (TTL) and complementary metaloxide-semiconductor (CMOS). The layout of the ground plane is shown in Fig. 3.

To steer the beam towards the front, back, left or right, the respective diode in this direction is configured as a director (i.e. OFF), while the remaining three diodes are configured as reflectors (i.e. ON). To steer the beam towards a diagonal direction, the two diodes in this direction are configured as directors (i.e. OFF), while the two diodes in the opposite direction are configured as reflectors (i.e. ON). The ESPAR can also be configured for joint front/back and left/right patterns, but these are not considered in this work.

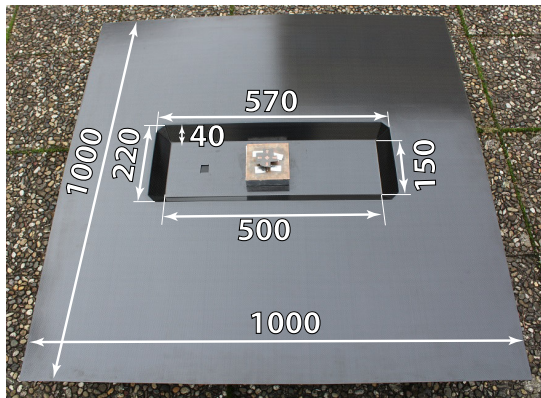
III. CHASSIS ANTENNA CAVITY

The antenna is flush-mounted in a chassis antenna cavity [11]. The cavity is built into the center $1\text{ m} \times 1\text{ m}$ carbon fiber reinforced polymer (CFRP) sheet, which acts as a chassis mockup. The CFRP sheet is built as a laminate with the autoclave method from plain weave prepregged fibers (prepreg). Eight fabric layers are stacked as $[(0^\circ/90^\circ)_4]$ to get a part thickness of about 2 mm. In the investigated frequency band the woven CFRP can be modeled as an isotropic conductor [19]. The same cavity geometry as in [11], [15], [16], [19] is used to keep comparability with previous results. The cavity has a rectangular shape with tilted walls. The cavity is 40 mm deep and its dimensions are $150\text{ mm} \times 500\text{ mm}$ on the cavity floor and 220×570 mm at the sheet.

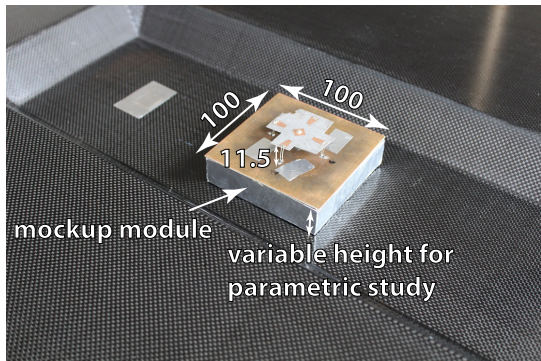
The cavity was not covered during the measurements. In practice the protective covers are not only designed due to antenna considerations, but also to meet mechanical and aesthetic requirements. The antenna evaluation would then depend on a specific selection of a cover geometry and material. This is undesired for a principal investigation, but a radome is expected to influence the antenna and should be considered for applications.

A. Antenna Height Sweep

The chassis antenna cavity is 40 mm deep, but due to the top-loaded monopole design, the ESPAR has a height of only



(a)



(b)

Fig. 4: a) Photograph of the ESPAR in the chassis antenna cavity. b) Closeup of the ESPAR on an electronics module mockup. All dimensions are in millimeter.

11.5 mm. This leaves space underneath the antenna, which could be used to move control and communication electronics close to the antenna and reduce cables from the roof to the car electronics [20]. Influences of antenna mounting height inside the cavity are investigated with measured gain patterns. For this purpose module mock-ups of different height are placed underneath the antenna during measurement. The mock-ups are made from hard-foam that is wrapped in adhesive aluminum foil. They have a hole in the center such that the bias-voltage and coaxial cables can be pulled through. The measured heights range from 0 mm (no mockup, ESPAR on cavity floor) to 25 mm in 5 mm steps.

IV. MEASUREMENT RESULTS

The measurements are performed in the anechoic chamber at Karlsruhe Institute of Technology. The chamber is a far-field measurement system. The pin-diodes are switched by connecting them to a DC power supply. The antenna and the chassis cavity are symmetric. Therefore, only patterns towards three directions are measured: front, diagonal and side. The antenna cavity is designed for automotive applications and for the following discussion it is considered that the module is mounted as depicted in Fig. 1 with its short side towards the front and its long side towards the side. The 0° state

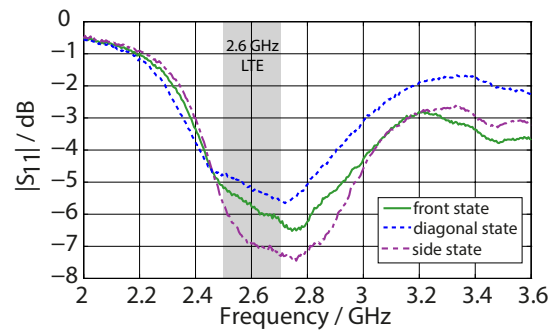


Fig. 5: Absolute value of the measured S-parameters.

then corresponds with the front of the car and the side state corresponds with the right side of the car.

The matching of the antenna is evaluated based on the absolute values of the measured scattering parameters. The return loss is about 5 dB or better in the 2.6 GHz LTE frequency bands 7 and 38. There is dependence on the selected state. In the diagonal state the return loss is reduced by 1 dB, which is within acceptable bounds. In comparison to the return loss without the cavity [18] small deviations are evident. Without the cavity the return loss in the diagonal state was slightly better than 6 dB and is therefore reduced by about 1 dB. The return losses of the front, back, left and right states were about 12 dB, but are reduced when the antenna is placed in the cavity. Moreover, while the antenna is symmetric for the front and side state, these return losses differ by 1 dB, which we speculate to be either a result of prototype production tolerances or coupling with the closer cavity wall in front direction.

Fig. 6 shows the measured gain patterns. The gain patterns in Fig. 6a show the vertical cuts towards the front (short cavity side). As expected, the gain towards the front is largest when the antenna is configured in front state and the gain is reduced when the antenna is configured in a diagonal or side state. The gain of the front state is ≥ 0 dBi for polar angles $45^\circ \leq \theta \leq 80^\circ$. The pattern is smooth in this area and no nulls are introduced by the cavity. The gain of the diagonal state is ≈ 1 dB lower than the front state and the pattern is also smooth. However, the back lobe of the front state is quite large and the gain of the front state towards the rear is almost as large as the gain towards the front. This is a direct influence of the cavity walls being closer to the antenna in this direction. The front/back gain difference is larger without the cavity (5 dB, compare [18]) and towards the longer side of the cavity, where the cavity walls are further away from the antenna (compare Fig. 6b). This problem could be accounted for by considering the cavity walls in a design iteration on the antenna, or by changing the cavity design to increase the distance between walls and antenna.

The vertical gain pattern cuts towards the sides are shown in Fig. 6b. The diagonal state has a gain ≥ 0 dBi from $30^\circ \leq \theta \leq 90^\circ$, a maximum gain of 8 dBi and 5 dB larger gain than the front state has in this direction. The gain of the diagonal

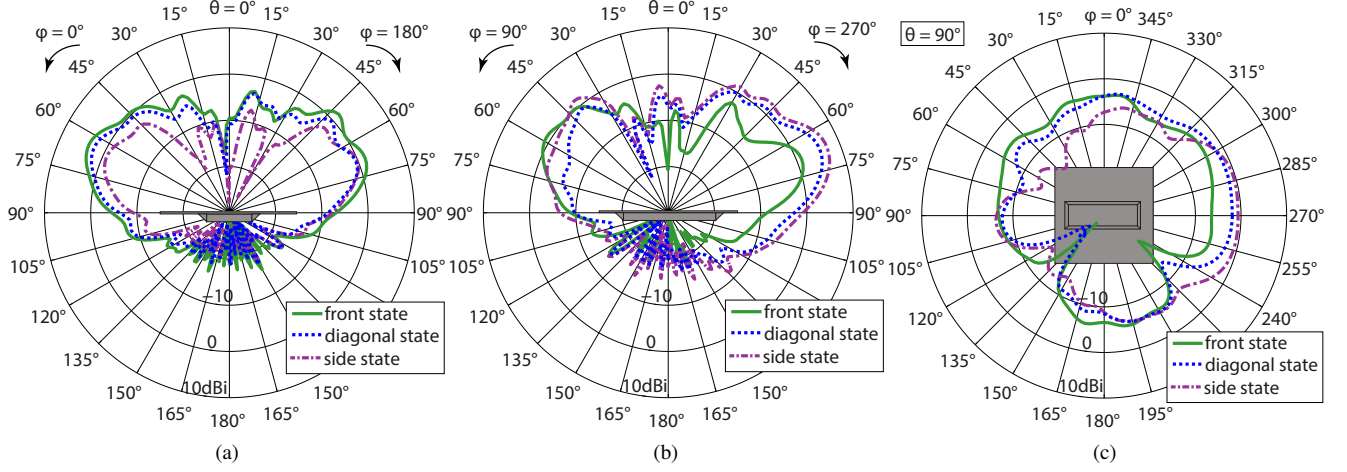


Fig. 6: Measured gain patterns at 2.6 GHz, vertical polarization, antenna on floor in cavity center, a) Vertical cuts towards the short side of the cavity ($\varphi = 0^\circ$ and 180° ; towards the front/back of the car when cavity is mounted according to Fig. 1). b) Vertical cuts towards the long side of the cavity ($\varphi = 90^\circ$ and 270° ; towards the sides of the car when cavity is mounted according to Fig. 1). c) Horizontal cuts for polar angle $\theta = 90^\circ$.

state is ≈ 2 dB lower towards the side than the gain of the side state. The flush-mounted performance in this direction is similar to the case when the antenna is used without cavity [18].

Fig. 6c compares the horizontal cuts of the gain patterns for polar angle $\theta = 90^\circ$, which corresponds with the plane of the CFRP chassis mockup. Generally, radiation patterns get pushed upwards, when an antenna is placed on a large ground plane. This sets the gain target at around 0 dBi in the horizontal plane for vehicles. Fig. 6c nicely illustrates the pattern reconfiguration between the different states. The antenna beam can be electronically steered by 45° with opening angles of about $\pm 30^\circ$. For the front state the gain is lower in the horizontal plane, which is again a result of the proximity to the walls on the short cavity side. The gain of the side state reaches 0 dBi and the gain of the directional state is larger than the front and side state gains for $310^\circ \leq \varphi \leq 345^\circ$.

Fig. 7 shows the results of the parametric study with variable height of the ESPAR in the cavity. The height of the electronics module mockup is given, which then also corresponds to the height at which the ESPAR is placed above the cavity floor. The gain around the horizontal plane is not significantly influenced by the mounting height. Most notably, two nulls in the gain pattern appear the further the antenna is elevated from the floor. on the floor the nulls start around $\theta \approx 15^\circ$ and move to 60° when the ESPAR is placed at the cavity opening.

V. CONCLUSION

Previous works [15], [16] showed that pattern reconfigurable antennas based on phased driven elements can be flush-mounted inside a chassis cavity. In this work it is demonstrated that ESPARs can be used in automotive applications with chassis cavities.

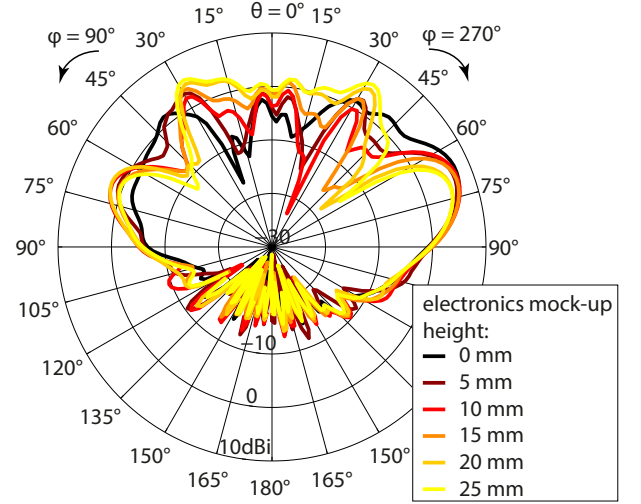


Fig. 7: Measured gain patterns for different heights of the electronics module mockup underneath the antenna; 2.6 GHz, vertical polarization, side state.

An electronically steerable parasitic array radiator (ESPAR) for the 2.6 GHz LTE frequency band is flush-mounted inside a rectangular chassis antenna cavity. The antenna retains its reconfiguration capabilities when flush-mounted, but the gain towards the short cavity side is improvable.

While the presented ESPAR is designed for the 2.6 GHz LTE band, it can be assumed that the same solution (flush-mounted ESPARs in chassis cavities) is feasible for other services with frequency bands in the same region, e.g. WLAN at 2.4 GHz or V2X at 5.9 GHz.

ACKNOWLEDGMENT

This work was supported by a STSM Grant from COST Action CA15104 IRACON. The financial support by the Austrian Federal Ministry of Education, Science and Research is gratefully acknowledged.

REFERENCES

- [1] R.L. Jesch, "Measured Vehicular Antenna Performance," *IEEE Transactions on Vehicular Technology*, vol. VT-34, no. 2, pp. 97-107, 1985.
- [2] A. Pal, A. Mehta, D. Mirshekar-Syahkal, and H. Nakano, "A Twelve-Beam Steering Low-Profile Patch Antenna With Shorting Vias for Vehicular Applications," *IEEE Transactions on Antennas and Propagation*, vol. 65, no. 8, 2017.
- [3] J. Kowalewski, I. Mehinovic, S. Abadpour, J. Mayer, and T. Zwick, "A Pattern Reconfigurable Antenna System for Automotive MIMO Applications," in *German Microwave Conference (GeMiC)*, Freiburg, Germany, 2018.
- [4] R.D. Zerod, G.F. Tannery, and M.-R.S. Movahhed, "Concealed antenna system with remote variable gain rf amplifier," U.S. Patent 5,428,830, 1995.
- [5] J.H. Schaffner, H.J. Song, A. Bekaryan, H.-P. Hsu, M. Wisniewski and J. Graham, "The Impact of Vehicle Structural Components on Radiation Patterns of a Window Glass Embedded FM Antenna," *IEEE Transactions on Antennas and Propagation*, vol. 59, no. 10, pp. 3536-3543, 2011.
- [6] J.H. Lee, S.H. Lee, D. Kim, and C.W. Jung, "Transparent antenna using a μ -metal mesh on the quarter glasses of an automotive for DMB service receiving," *Microwave and Optical Technology Letters*, 2018, DOI: 10.1002/mop.31441.
- [7] E. Gschwendtner, and W. Wiesbeck, "Ultra-Broadband Car Antennas for Communications and Navigation Applications," *IEEE Transactions on Antennas and Propagation*, vol. 51, no. 8, pp. 2020-2027, 2003.
- [8] J. Tak, and J. Choi, "A flush-mounted monopolar patch antenna for UAV applications," *Microwave and Optical Technology Letters*, vol. 59, no. 5, pp. 1202-1207, 2017.
- [9] S. Lee, G. Jeoung, and J. Choi, "Three-dimensional-printed tapered cavity-backed flush-mountable wideband antenna for UAV," *Microwave and Optical Technology Letters*, vol. 59, pp. 2975-2981, 2017.
- [10] N. Nguyen-Trong, S.P. Pinapati, D. Hall, A. Piotrowski, and C. Fumeaux, "Ultralow-Profile and Flush-Mounted Monopolar Antennas Integrated Into a Metallic Cavity," *IEEE Antennas and Wireless Propagation Letters*, vol. 17, pp. 86-89, 2018.
- [11] G. Artner, R. Langwieser, and C.F. Mecklenbräuker, "Concealed CFRP Vehicle Chassis Antenna Cavity," *IEEE Antennas and Wireless Propagation Letters*, vol. 16, pp. 1415-1418, 2017.
- [12] G. Artner, W. Kotterman, G. Del Galdo, and M.A. Hein, "Conformal Automotive Roof-Top Antenna Cavity With Increased Coverage to Vulnerable Road Users," *IEEE Antennas and Wireless Propagation Letters*, 2018, DOI: 10.1109/LAWP.2018.2876628.
- [13] I.M. Yousaf, and B.K. Lau, "On Performance of Hidden Car Roof Antennas," in *European Conference on Antennas and Propagation (EuCAP)*, London, England, 2018.
- [14] S. Zwickl-Bernhard, J. Steiner, A. Pöllinger, and G. Artner, "Carbon-Fiber Reinforced Antenna Cavity Hidden in the Monocoque of a Racing Car," in *IEEE International Symposium on Personal, Indoor and Mobile Radio Communications (PIMRC)*, Bologna, Italy, 2018.
- [15] G. Artner, J. Kowalewski, C.F. Mecklenbräuker, and T. Zwick, "Pattern Reconfigurable Antenna With Four Directions Hidden in the Vehicle Roof," in *International Workshop on Antenna Technology (iWAT)*, Athens, Greece, 2017.
- [16] G. Artner, J. Kowalewski, C.F. Mecklenbräuker, and T. Zwick, "Automotive Pattern Reconfigurable Antennas Concealed in a Chassis Cavity," in *International Symposium on Wireless Personal Multimedia Communications (WPMC)*, Yogyakarta, Indonesia, 2017.
- [17] E. Safin, R. Valkonen, and D. Manteuffel, "Reconfigurable LTE MIMO Automotive Antenna System Based on the Characteristic Mode Analysis," *European Conference on Antennas and Propagation (EuCAP)*, Lisbon, Portugal, 2015.
- [18] J. Kowalewski, J. Atuegwu, J. Mayer, T. Mahler, and T. Zwick, "A Low-Profile Pattern Reconfigurable Antenna System for Automotive MIMO Applications," *Progress in Electromagnetics Research*, vol. 161, pp. 41-55, 2018.
- [19] G. Artner, P.K. Gentner, R. Langwieser and C.F. Mecklenbräuker, "Simulation Model for Chassis Antenna Cavities Made from Carbon Fiber Reinforced Polymer," in *European Conference on Antennas and Propagation (EuCAP)*, London, United Kingdom, 2018.
- [20] M. Geissler, K. Scharwies, and J. Christ, "Intelligent Antenna Systems for Cars," in *German Microwave Conference (GeMiC)*, Aachen, Germany, 2014.